# 1 One-pot generation of lignin microspheres and digestible substrate

- 2 with a polyol-DES pretreatment in high solid loading
- 3 Jinyuan Cheng<sup>a</sup>, Yunni Zhan<sup>a</sup>, Xuze Liu<sup>a</sup>, Chen Huang<sup>a,\*</sup>, Xuelian Zhou<sup>a,\*</sup>, Jia Wang<sup>b</sup>,
- 4 Xianzhi Meng<sup>c</sup>, Chang Geun Yoo<sup>f</sup>, Guigan Fang<sup>a,\*</sup>, Arthur J. Ragauskas<sup>c,d,e</sup>
- <sup>a</sup>Institute of Chemical Industry of Forest Products, Chinese Academy of Forestry,
- 6 Jiangsu Province Key Laboratory of Biomass Energy and Materials, Nanjing 210042
- <sup>7</sup> Co-Innovation Center for Efficient Processing and Utilization of Forest Resources,
- 8 Nanjing Forestry University, Nanjing 210037, China
- <sup>9</sup> Department of Chemical and Biomolecular Engineering, University of Tennessee
- 10 Knoxville, Knoxville, TN 37996, USA.
- dDepartment of Forestry, Wildlife, and Fisheries, Center for Renewable Carbon, The
- 12 University of Tennessee Institute of Agriculture, Knoxville, TN 37996, USA.
- 13 <sup>e</sup>Joint Institute for Biological Science, Biosciences Division, Oak Ridge National
- Laboratory, Oak Ridge, TN 37831, USA.
- 15 fDepartment of Paper and Bioprocess Engineering, State University of New York
- 16 College of Environmental Science and Forestry, Syracuse, New York 13210-2781,
- 17 United States.

# 19 Abstract

- 20 Previous lignin microspheres (LMS) preparation needs multiple steps with very
- 21 low yield and high cost. Herein, we developed a high-solid deep eutectic solvent
- 22 (DES) pretreatment for an effective lignin fractionation and enzymatic

saccharification of moso bamboo under mild temperature (110 °C) with high solid loading. Lignin was significantly removed from the plant cell wall, and cellulose properties (e.g., crystallinity and degree of polymerization) were also altered during the pretreatment. As a result, the enzymatic digestibility of the pretreated bamboo was dramatically increased. Uniform micro-spherical lignin was directly produced from the pretreatment system, and its particle size could be regulated by controlling the solid loadings and pretreatment temperatures. The lignin microspheres formation mechanism was investigated by analyzing the lignin's size distribution, molecular weight distribution, chemical structure, and hydrophobicity. The DES showed excellent recyclability, and the recycled DES could still remove 42.78% lignin even after 7th circulation associated with 100% glucan saccharification. The mass balance based on 1000 g biomass showed that 196.28 g LMS was directly recovered, which exhibited a high RhB adsorption. Besides, 404.91 g glucose and 36.67 g xylose were obtained after the enzymatic saccharification process. Specifically, GAPI analysis exhibited a near total green and yellow portions of the pictogram, indicating our DES process was green enough to make this biorefinery sustainable. Overall, the proposed DES generated synergistic productions of digestible solid and LMS which could contribute to establish a green and sustainable biorefinery sequence with diverse outputs in one pot. **Keywords**: Deep eutectic solvents, Delignification, Enzymatic hydrolysis, Lignin

## 1. Introduction

microspheres, High-solid pretreatment

23

24

25

26

27

28

29

30

31

32

33

34

35

36

37

38

39

40

41

42

43

Lignocellulosic biomass, which is mainly composed of cellulose, hemicellulose, and lignin, is the most abundant renewable feedstock on the earth. It has received significant attention for its ability to produce materials, fuels, and chemicals through the biorefinery process (Lancefield et al., 2017). For a conventional biorefinery platform, the processing of biomass is hampered by the compact physical and chemical structures of lignocellulosic biomass (Xu et al., 2020). Lignin is a complex and heterogeneous natural macromolecule containing various phenolic monomers (e.g., p-hydroxyphenyl, guaiacyl, and syringyl) bonded by a series of C-O and C-C linkages such as  $\beta$ -O-4,  $\beta$ - $\beta$ , and  $\beta$ -5 bonds. It acts as the vital glue endowing biomass their structural integrity and mechanical strength. Lignin is recognized as the key recalcitrant component in the biorefinery process (Mankar et al., 2021). In conventional pulping processes, lignin is often treated as a low-value combustion fuel, however in recent years, it has an increasing market value as a renewable alternative to replace petrochemicals such as phenolic compounds and nano/micro materials (Ragauskas et al., 2014). This interest necessitates the efficient isolation and preparation of a clean lignin stream with high reactivity and integrity. In the past two decades, many pretreatment methods, such as sulfite, auto-hydrolysis, alkali, dilute acid, and alkaline hydrogen peroxide, have been developed to convert lignocellulose to biofuel effectively (Lancefield et al., 2017). While these methods can yield a satisfying cellulose-to-glucose conversion, the quantity and quality of the lignin fraction generated from many of these processes are not considered as much as cellulose. This is mainly because the recovered lignin from these methods often

45

46

47

48

49

50

51

52

53

54

55

56

57

58

59

60

61

62

63

64

65

suffers from high impurity, low reactivity, high condensation, low yield, and wide polydispersity, making it difficult to further valorize into useful chemicals or materials (Abu-Omar et al., 2021).

67

68

69

70

71

72

73

74

75

76

77

78

79

80

81

82

83

84

85

86

87

88

Deep eutectic solvent (DES) is an emerging ionic liquid-like solvent that possesses biocompatibility, biodegradability, recyclability, and shows high efficiency for lignocellulose pretreatments (Huang et al., 2021). DES comprises hydrogen-bond donors (HBD) and hydrogen-bond acceptors (HBA) through hydrogen bond interactions (Sánchez-Camargo et al., 2019). The strong H-bond between HBD and HBA makes the solvent strong enough to complete with the inner linkages in biomass and lead to the cleavage of H-bonds, glycosidic bonds and ether bonds to fractionate the lignocellulose (Xia et al., 2018). Although DESs effectively remove lignin and hemicellulose, some inherent problems still hinder their future industrial applications. For instance, the recovered DES lignin typically suffered from severe structural degradation and condensation even at a mild condition when pretreated with the carboxylic acid-based DES, such as using maleic acid, formic acid, lactic acid, and oxalic acid as the HBD (Hong et al., 2020). Thus, most lignin recovered from the abovementioned DES systems has limited applications. Another problem associated with DES pretreatment is its high viscosity, which typically requires a high DES dosage to accelerate mass transfer. Some studies explored the high-solid DES pretreatment (Modenbach and Nokes, 2012), but multiple steps are inevitable. For example, Chen et al. performed an ethylene glycol-based DES pretreatment at a 27% biomass loading, and the results showed that a glucose yield of 90% at 130 ° C

could be achieved (Chen et al., 2018a). Ai et al. further increased the solid loading to 50% using a glycerin-based DES mediated extrusion system which achieved ~76.4% cellulose conversion l at the pretreatment temperature of 180 ° C (Ai et al., 2020). Despite the relatively high glucose yields, these pretreatments still need high temperatures/long pretreatment time to fractionate the lignocellulose, and possible lignin valorization routes were not explored. To facilitate the fractionation ability, catalyst-promoted polyol-based DES systems have also been widely investigated. For example, Xia et al. (Xia et al., 2018) found that the AlCl<sub>3</sub>·6H<sub>2</sub>O catalyzed ChClglycerol system could significantly improve the lignin fractionation efficiency from 3.61% to 98.46%. Wang et al. (Z. K. Wang et al., 2020) have also investigated the Lewis acid-catalyzed and polyol-based DES pretreatment which could dramatically enhance the fractionation ability. However, the lignin valorization was neglected during these DES pretreatment processes. It could be argued that the lignin isolation and its utilization have become a key point restricting large-scale DES application. Lignin microsphere (LMS) synthesis is one of the most attractive lignin valorization approaches. Over the past few years, LMS has been widely investigated in sewage treatment agents, cosmetics, and polymeric applications (Österberg et al., 2020). LMS preparation is quite susceptible to its inherent structural characteristics, such as molecular weight, polydispersity, and hydrophobicity (Ma et al., 2020). The LMS preparation methods often need multiple steps, including acid precipitation, dialysis, chemical modification, and coordination, which result in extended processing time, low yield, high cost, and environmental contamination (often using

89

90

91

92

93

94

95

96

97

98

99

100

101

102

103

104

105

106

107

108

109

environmental hazardous chemicals in chemical modification and acid precipitation processes) (Österberg et al., 2020). Pang et al. (Pang et al., 2020) proposed a solventanti-solvent method for LMS precipitation using the enzymatic hydrolysis lignin which could obtain a series of uniform LMS, but need a tedious lignin isolation process, long preparation time, toxic solvent and high cost. Besides, Chen et al. (Chen et al., 2020) successfully prepared uniform LMS using the chip and abundant alkaline and kraft lignin, while this process needed time consuming processes of anti-solvent precipitation and dialysis which greatly constrain its scale-up. To make LMS economically feasible, significant modification of processing is essential. This study aims to develop a high-solid loading pretreatment approach under mild condition (low temperature of 110 °C, less time of 1 h and high SLR) using a ternary ChCl/1,4butanediol (BDO)/AlCl<sub>3</sub> DES system, which applied raw lignocellulosic biomass as the starting material for uniform LMS production while preserved most carbohydrates for the monosaccharides production in the subsequent enzymatic hydrolysis. As contrast, we also studied the lignin properties recovered from organic acid-based DES and other polyol-based DESs. The results showed that the polyol-based DES system could uniquely yield uniform LMS after the pretreatment, while the lignin recovered from the organic acid-based DES all exhibited irregular shape which is covered by a large amount of lignin debris. The possible mechanism of the LMS formation during the pretreatment was also proposed. A combination of scanning electron microscope (SEM), X-ray diffraction (XRD), two-dimensional heteronuclear single quantum coherence nuclear magnetic resonance (2D HSQC NMR), and Zeta-sizer analysis

111

112

113

114

115

116

117

118

119

120

121

122

123

124

125

126

127

128

129

130

131

were applied to evaluate the impact of high solid DES pretreatment on the structural and chemical variations of bamboo components as well as the physical characteristics of the LMS particles. Our study demonstrated the great potential of the BDO DES pretreatment in valorizing the cellulose and lignin fractions in lignocellulosic biomass, yielding fermentable sugars and LMS as synergistic products in one pot, which could solve the problems of tedious processes, low yield, and high cost in conventional LMS preparation process.

#### 2. Materials and methods

#### 2.1. Materials

The bamboo feedstock (moso bamboo) provided by Xianhe Paper Industry (Zhejiang Province, China) was crushed with a twin-extruder, and the crushed bamboo was air-dried (with a final water content of 7.62%) and then stored in a zip bag for further use. The air-dried moso bamboo shaped as fibril agglomerates, and the fibril size was measured to be in 3-5 mm long and 0.3-1 mm wide. Cellulase (SAE 0020, 250 FPU/g) and xylanase (X2753, 3490 U/g) were purchased from Sigma-Aldrich (Shanghai, China). Choline chloride (ChCl) was obtained from Machlin Biochemical Co., Ltd, (Shanghai, China). 1,4-butanediol (BDO), AlCl<sub>3</sub>, and other chemicals were purchased from Sinopharm Chemicals reagents (Beijing, China).

2.2. DES preparation and pretreatment

Considering the poor performance solely applying polyol-based DES such as ChCl/glycerol (Xia et al., 2018) and ChCl/glycol (Hong et al., 2020), here we introduced trace AlCl<sub>3</sub> as the catalyst to strengthen the fractionation ability. The DES

was prepared by mixing ChCl, BDO, and AlCl<sub>3</sub> (using a 25:50:1 molar ratio) at a three-neck flask. Then, the mixture was reacted in a glycerin bath (90 °C) with consecutive agitation to form a homogeneous and transparent liquid, finally it was put into a desiccator before pretreatment. It was found that the DES turned into solid state at temperature < 20°C, thus the DES was preheated at 50 °C prior to the pretreatment. In the pretreatment process, 10 g feedstock (dry weight) was blended with the DES at different solid to liquid ratios (SLR, w/w) of 1:1, 1:2, 1:4, 1:6, 1:8, and 1:10 at a mild temperature of 110 °C. The pretreatment was carried out at different temperatures (e.g., 90, 100, 110, 120, and 130 °C) for 1 h with consecutive agitation in an oil bath. Once the pretreatment was finished, 300 mL of 50 v/v% acetone/water solution was introduced to quench the reaction, followed by magnetic stirring for 2 h. Next, the solid and liquid separation was conducted by vacuum filtration. The solid was washed twice with another 200 mL fresh acetone/water solution, then washed with excessive DI water until the effluent was neutral pH and stored at 4 °C before analysis. The lignin-rich filtrate was gathered, and then rotary-evaporated (50 °C) to remove the acetone, followed by adding 750 mL of DI water to precipitate the lignin. The precipitated lignin was centrifugally recovered, washed with DI water to neutral pH, and freeze-dried to obtain the solid lignin sample. The yield of recovered lignin was calculated based on the ratio of the precipitated lignin (weight) over the removed lignin during the pretreatment. All experiments in our study were performed in duplicate. After the lignin precipitation, the DES was recovered by evaporating the water at 70 °C using a rotary evaporator, and the obtained DES was weighted to

155

156

157

158

159

160

161

162

163

164

165

166

167

168

169

170

171

172

173

174

175

- determine the recovery yield.
- 178 2.3. Characterizations
- 179 2.3.1 Enzymatic hydrolysis
- The enzymatic hydrolysis experiment was performed at a 2.5% solid 180 181 loading (w/v) according to a previous publication (Huang et al., 2021). In brief, 182 about 500 mg dry weight of sample was weighed into the glass flask, then 1 mL 183 acetate buffer (1 M) was introduced to control the pH ~4.8. Cellulase (25 FPU/g-glucan) and xylanase (150 U/g-xylan) were followed. After 184 185 supplementing DI water to a total volume of 20 mL, the mixture was put into a 186 shaking incubator (150 rpm, 50 °C) for 72 h. Once the incubation finished, 1 187 mL of sample was withdrawn to quantify the sugars release by the high-188 performance liquid chromatography (HPLC). The equation of calculating the 189 enzymatic hydrolysis yield was shown as follows:
- Enzymatic hydrolysis yield (%) =  $\frac{\text{Glucose/xylose in the enzymatic hydrolyzate (g)}}{\text{I}_{\text{nitial glucan/xylan in the substrate (g)}} \times 1.11/1.14}$
- 192 2.3.2 Substrates characterizations

191

193

194

195

196

197

The chemical composition determination of raw and pretreated bamboo substrates was referred to the National Renewable Energy Laboratory (NREL) protocol (Sluiter et al., 2012), and the detailed procedures could be found in our recent study (Cheng et al., 2022). The monomeric sugars, furfural and acetic acid in this study were quantified by HPLC (Agilent 1260 II). Different

100%

- monosaccharides were separated by an HPX-87H column (Bio-Rad Aminex)
- with 5 mM sulphuric acid as the mobile phase (0.6 mL/min at 55 °C).
- 200 X-ray diffraction (XRD) test was performed on a Bruker D8
- 201 diffractometer (Bruker, Germany) using a Cu-Kα X-ray generator (40 kV, 40
- 202 mA). The sample testing was scanned from  $10^{\circ}$  to  $40^{\circ}$  ( $2^{\circ}$ /min). The
- 203 crystallinity index (CrI) calculation was based on the following equation:
- 204  $\operatorname{CrI} = \frac{[I_{002} I_{am}]}{I_{002}} \times 100$
- Where  $I_{002}$  (at around 22°) represents the maximum intensity of diffraction peak,
- and  $I_{am}$  (at around 18°) represents the minimum intensity of the amorphous
- 207 proportion.
- 208 Cellulose DP<sub>v</sub> experiment was referred to a viscosity procedure of the ISO 5351
- standard, and the detailed procedure could be referred to previous publications (Sirviö
- 210 et al., 2016).
- 2.3.3 Lignin characterization
- The lignin recovery yield was obtained based on the regenerated lignin from
- 213 pretreatment liquid and the total removed lignin from bamboo, and the corresponding
- 214 calculation equation was shown as follows.
- Lignin yield (%) =  $\frac{\text{Lignin recovered from the pretreatment liquid (g)}}{\text{Total removed lignin from the initial bamboo (g)}} \times 100\%$
- The proportion of carbohydrates in the recovered lignin was determined by two-
- step acid hydrolysis referred to the abovementioned NREL protocol. According to a
- 218 previous publication, CEL (cellulolytic enzyme lignin) of raw bamboo was extracted
- by consecutive enzymatic hydrolysis and dioxane extraction (Wen et al., 2015).

The surface characteristics and microstructural changes of lignin were imagined
by a field emission scanning electron microscopy (FE-SEM, S-3400N II, HITACHI
Company, Japan) operated at a 10 kV acceleration voltage. The samples were sprayed
by gold before the test.

The molecular weights analysis was analyzed by GPC (gel permeation chromatography). Before the GPC test, the samples were acetylated using pyridine and anhydride (1:1, v/v) at RT for 24 h. After acetylation, the acetylated samples (4 mg) were readily dissolved in THF (2 mL) to reach a concentration of 2 mg/mL for molecular weight analysis by GPC using a UV detector at 240 nm.

2D-HSQC NMR experiments were conducted by a Bruker Ascend<sup>TM</sup> 600 MHz spectrometer. Before test, around 150 mg lignin sample was dissolved in 0.6 mL DMSO-d6, and the detailed procedures and acquisition parameters could be found in our previous publication (Cheng et al., 2022).

The average microsphere diameter (Z-Ave) and size distribution of the recovered lignin were analyzed using a Zeta-sizer (Nano ZS, Malvern Instrument, UK). The lignin sample was prepared at a concentration of 1 g/L and then sonicated for 10 min to disperse lignin in water prior to the analysis. It is believed that 10 min sonication treatment can effectively disperse lignin in the water, while extensive sonication treatment may cause reduction in the diameter (Ma et al., 2019).

Hydrophobicity of the recovered lignins was measured by the Rose Bengal assay (Wu et al., 2018). In brief, different amounts of recovered lignin (6, 12, 18, 24, 30 mg) were weighed into 15 mL citrate buffer (0.05 M, pH~4.8) with 0.03 M Rose

Bengal. Then, the mixture was transferred into a shaking incubator (50 ° C, 150 rpm) and incubated for 2 h. At the end of incubation, the mixture was centrifuged (9000 rpm, 10 min) for solid-liquid separation. After that, the residual Rose Bengal in the liquid was determined by UV-Vis spectrometer at 543 nm. The dye adsorption quantity was calculated according to the difference of free dye in the solution of the initial and equilibrated adsorption process. Partition quotient (PQ) is defined as the ratio of the amount of absorbed dyes over the residual free dyes, which is linearly fitted with the corresponding sample concentration, and the slope represents the surface hydrophobicity of recovered lignin.

2.3.4 Organic dye removal test

The adsorption capacities of the LMS toward organic dye Rhodamine B (RhB) were performed to evaluate the potential of the LMS as a contaminant remover. To provide a theoretical basis for practical application, this study adopted the RhB with concentrations of 150 mg/L, and the test was performed in a shaker (40 °C, 110 rpm) for 24 h (Li et al., 2016). After 24 h adsorption, the LMS were removed from the suspension by centrifugation (6000 rpm, 15 min). Kinetic analysis for RhB dyes was performed by applying 50 mg LMS in 25 mL of the RhB solution (150 mg/L) under 40 °C. The RhB concentration in the solution was periodically quantified with a UV-vis spectrophotometer at 554 nm.

The adsorption capacity (q<sub>e</sub>, mg of dye/g of adsorbent) of RhB dye was determined by the following equation:

$$263 \qquad q_e = \frac{(c_0 - c_e) \times v}{m}$$

Where  $c_0$  (mg/L) and  $c_e$  (mg/L) represent the initial and equilibrium concentrations of the RhB; v (L) and m (g) are the volume of aqueous solution and the weight of adsorbent.

#### 3. Results and discussion

- 3.1 Substrates characterization
- 3.1.1 Chemical composition analysis
- Pretreatments under different molar ratios were fist conducted to optimize the AlCl<sub>3</sub> addition, and the result showed that the fractionation ability slightly increased with the AlCl<sub>3</sub> molar proportion increased, while it nearly reached a plateau at the molar ratio of 25:50:1 (data is not shown). Considering the cost, here we chose the fixed ChCl/BDO/AlCl<sub>3</sub> of 25:50:1 as the experimental condition.
- After pretreatment under different SLRs (1:1-1:10) and different temperatures (90-130 °C), the recovery yields of the pretreated solid, glucan, xylan, and the lignin removal in different pretreatments are shown in Fig. 1. As shown in Fig. 1a, even at a very high solid to liquid ratio (SLR) of 1:1 (110 °C), only 74.03% solid was recovered, indicating the efficient pretreatment even under the highest SLR. With decreasing SLR, solid yield continued to decrease, dropping from 74.03% to 65.28% (1:2) and 59.24% (1:4), and a further decrease in SLR had a negligible impact on the solid recovery. It can be seen that the hemicellulose and lignin removal was the main reason causing the degradation of bamboo, as 42.60% xylan was retained in the solid and more than 38% lignin was removed, while glucan recovery remained very high (92.84%) at 1:1 SLR. As the SLR decreased to 1:4, the xylan recovery decreased, and

lignin removal increased, which were 27.03% and 69.72%. When further decreasing the SLR (1:4~1:10), the lignin removal and xyaln recovery almost remained constant (within 10% variation). After balancing the lignocellulose fractionation efficiency and the cost, we selected the optimum SLR of 1:4 to conduct further study. In contrast, the glucan recovery stayed relatively high during all the process, which had a yield of ~90%, indicating that glucan was well-preserved during the DES pretreatment. The effect of pretreatment temperatures on the biomass composition was also investigated at 20% solid loading (i.e., 1:4 SLR). As shown in Fig. 1b, the solid yield decreased gradually from 82.1% to 56.9% as the temperature increased from 90 to 120 °C. In comparison, a further increase in pretreatment temperature to 130 °C slightly increased the solid yield to 59.39%. Xylan recovery significantly decreased from 67.49% to 1.78% as temperature increased from 90 to 130 °C. Lignin removal initially increased as the temperature was raised, and it reached the highest of 74.17% at 120 °C. Then the lignin removal decreased to 56.47% at a higher temperature of 130 °C, which might partially contribute to the increased solid recovery at this temperature. This result indicated the possible formation of pseudo lignin induced by the carbohydrates decomposition and the condensation of small lignin moieties under high-temperature DES pretreatment, which precipitated on the surface of the substrates (Y. Wang et al., 2020). Nevertheless, around 90% glucan through the

286

287

288

289

290

291

292

293

294

295

296

297

298

299

300

301

302

303

304

305

pretreatments was maintained, even at high temperatures.

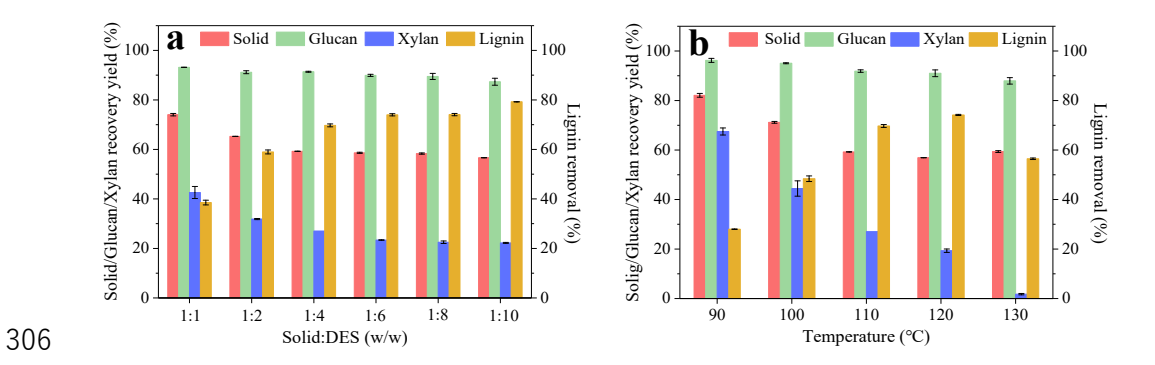


**Fig. 1.** Detailed components variations under different SLRs at 110 °C (a) and temperatures (b) under 1:4 SLR.

3.1.2. The crystalline index (CrI) and  $\text{DP}_{\nu}$  (cellulose degree of polymerization) analysis

The effects of pretreatment SLR (1:1-1:10) and temperature (90-130 °C) on the CrI and DPv were analyzed and the results are provided in Fig. 2. The CrI of raw bamboo was 59.63%, and it gradually increased to 66.91% (1:10 SLR) as the SLR decreased to 1:10 (110 °C, Fig. 2a), which was mainly induced by the degradation of amorphous hemicellulose and lignin. As to the effect of temperature (Fig. 2b), the CrI initially increased from 59.14% (90 °C) to the highest of 64.86% (120 °C), further increase of the temperature to 130 °C slightly decreased the CrI back to 63.55%. This result might be ascribed to the significant increase of DES permeation into the cellulose crystalline zone at severe temperature that caused its further swelling (Wu et al., 2018). The lignin condensation under the severe pretreatment condition at 130 °C caused the increase of lignin content and may also result in the CrI decrease.

For the DP<sub>v</sub> analysis, it was 773 for raw bamboo, which dramatically decreased

to 396 (a 49% reduction) upon being subjected to the DES pretreatment (1:1 SLR and

110 °C). The cellulose  $DP_v$  further reduced to 261 as the SLR decreased to 1:10 (Fig. 2a). A similar trend was observed in the DES pretreatment at different temperatures (Fig. 2b). These results revealed that although glucan recovery remained relatively constant during the DES pretreatment, the inner  $\beta$ -1,4-glucosidic bonds suffered from significant degradation, exposing more cellulose-reducing ends that may facilitate the subsequent enzymatic hydrolysis.

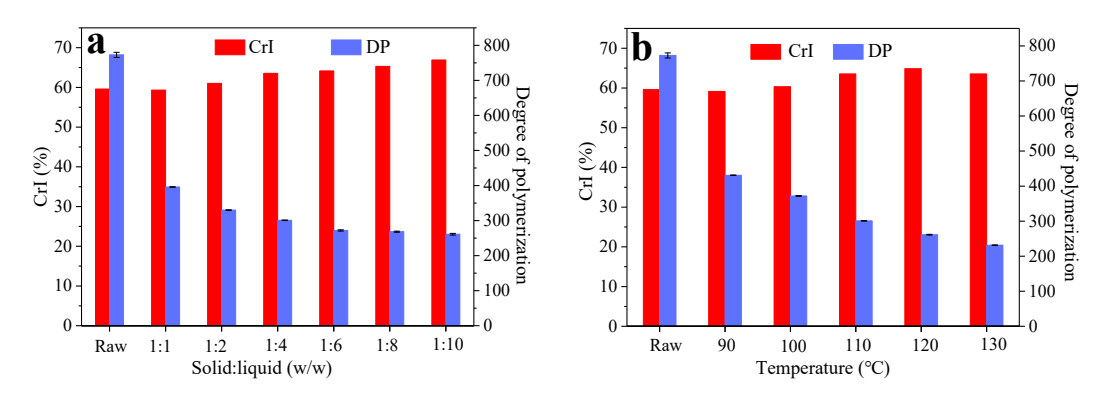


**Fig. 2.** The CrI and cellulose  $DP_v$  of the raw and pretreated bamboo at different SLRs at 110 °C (a) and different temperatures (b) under 1:4 SLR.

## 3.1.3. Enzymatic saccharification

Enzymatic saccharification of raw and pretreated bamboo samples under different conditions were conducted and compared in this section. To better assess the enzymatic hydrolysis performance of the pretreated solid, here we chose the commonly used solid loading of 2.5% in the enzymatic hydrolysis process. As shown in Fig. 3a, only 12.63% glucan saccharification yield and 1.74% xylan saccharification yield was obtained for raw bamboo. After the pretreatment, the glucan saccharification yield increased to 70% at the high SLR of 1:1, indicating our proposed DES can perform well at extremely high solid loadings. The glucan

saccharification yield at 1:2 SLR was higher than 90%, and a near 100% saccharification yield could be achieved with an SLR lower than 1:4. The xylan hydrolysis also had the same trend which showed the yield increased from 1.74% (raw bamboo) to 95.22% (SLR 1:2) and 100% (SLR of 1:4 or lower). As previously identified and widely reported in the literature, low SLR will increase the cost of pretreatment and solvent recovery processes, thus we chose the 1:4 SLR ratio as the optimized loading condition based on the high lignin removal and satisfying enzymatic saccharification. As to the temperature, the glucan saccharification reached its maximum (100%) at only 110 °C (Fig. 3b). Besides, enzymatic hydrolysis under higher solid loadings also performed and it showed a decreased enzymatic hydrolysis yield (data are not shown). In conclusion, the proposed high solid loading DES pretreatment system is capable of converting nearly 100% carbohydrate of the pretreated bamboo to their corresponding monosaccharides (e.g., glucose and xylose) through enzymatic hydrolysis, outperforming other DES systems such as ChCl/oxalic acid (58.5% glucose yield under 1:10 SLR at 160 °C) (Ling et al., 2021), benzyl triethylammonium chloride (BTEAC)/formic acid (76.64% glucan saccharification yield under 1:10 SLR at 130 °C) (Zhaohui Zhang et al., 2022), and BTEAC/lactic acid (LA) (72.5% glucose yield under 1:20 SLR at 120 °C for 2 h) (Guo et al., 2019), which usually need high pretreatment severity and low SLR. Because of the applied low pretreatment temperature, the DES solubilized lignin could avoid significant condensation reaction which will be demonstrated in the following section.

342

343

344

345

346

347

348

349

350

351

352

353

354

355

356

357

358

359

360

361

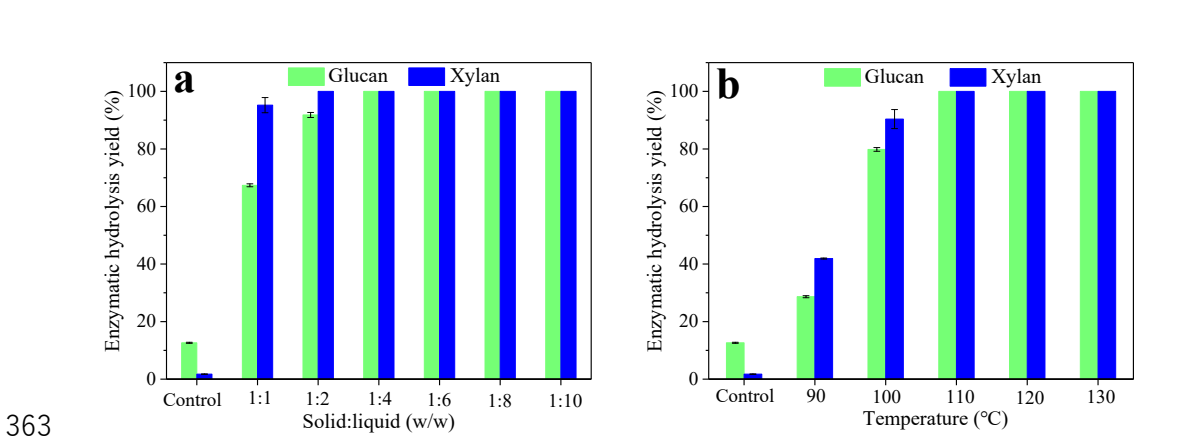


**Fig. 3.** 72 h saccharification yields under different SLRs (a) 110 °C and temperatures (b) under 1:4 SLR.

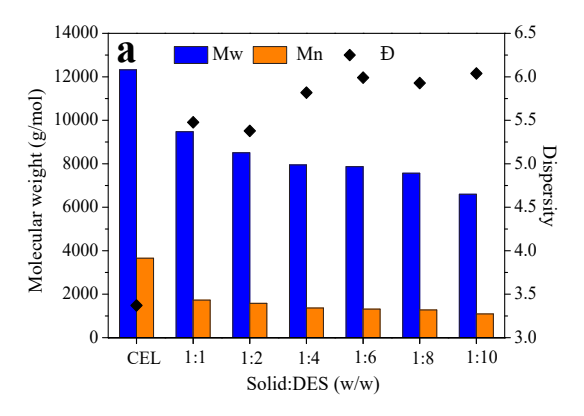
### 3.2 Lignin characterization

The dissolved lignin was then precipitated from the pretreatment liquid by adding sufficient water to destroy the hydrogen bond between HBD and HBA (Provost et al., 2022), and the lignin recovery yield based on the removed lignin was shown in Table S1. It can be seen that the lignin recovery yield was over 90% in most runs (except that at 1:1 SLR), higher than that achieved by typical alcohol pretreatment (Lancefield et al., 2017), ionic liquid/p-toluenesulfonic acid pretreatment (Wei et al., 2021), dioxane and methanol solution/HCl pretreatment (Pan et al., 2021), and tetrahydro-2-furanmethanol pretreatment (Xu et al., 2019). This is because that the bamboo lignin did not undergo severe depolymerization and exhibited a relatively intact structure which will be demonstrated in the following section. This result indicated that our recovered lignin exhibited a well-preserved structure which is liable to be recovered. Further, Zhang et al. have reported that the diol-grafted lignin structure intermediate was abundant after the diol-stabilized acidolysis (Zhenlei Zhang et al., 2022). Liu et al. (Liu et al., 2021) also found the diol (ethylene glycol)

could substantially graft onto the lignin side chains after a ternary DES pretreatment system. This grafting reaction might also contribute to the high recovery yield of lignin. This result indicated that high-purity lignin was obtained in a simple manner which favored the subsequent structural analysis and further valorization of such lignin.

# 3.2.1 Structural analysis of the recovered lignin

After pretreatment under different SLRs (at 110 °C) and different temperatures (under 1:4 SLR), the weight-average (M<sub>w</sub>), number-average (M<sub>n</sub>) molecular weights, and the dispersity of the recovered lignins are shown in Fig. 4. The raw bamboo CEL has an M<sub>w</sub> of 12322 g/mol. After DES pretreatment, M<sub>w</sub> of the recovered lignin decreased substantially, and it tends to be lower with lower SLR (from 9474 to 6800 g/mol) and high temperature (from 9415 to 6049 g/mol), which is ascribed to the enhanced DES permeation and bond cleavage at these conditions. The dispersity of the recovered lignin was increased after the pretreatment, which has also been reported in other DES pretreatment (Ai et al., 2020). This result can be explained by the fact that lignin underwent depolymerization and repolymerization, resulting in wider molecular size distribution.



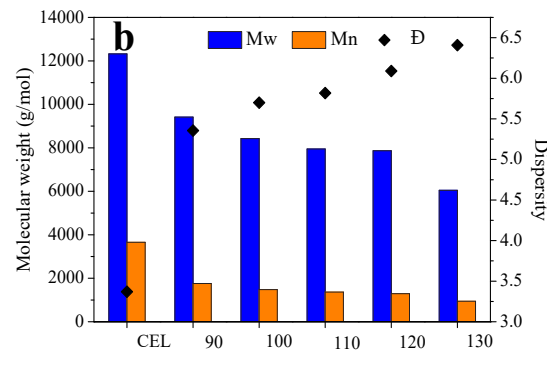


Fig. 4. Molecular weight and dispersity of CEL, and recovered lignins after DES pretreatment under different SLRs (a) at 110 °C and temperatures (b) under 1:4 SLR. Considering the plateaued fractionation ability (69.75% lignin removal and 91.38% glucan recovery), high carbohydrates saccharification, and high lignin recovery yield under the mild condition (110 °C, 1:4 SLR), here we choose this condition to unveil its structure after the DES pretreatment to provide a reference to valorize such lignin. The detailed chemical structure of the CEL and recovered lignin (at 20% solid loading and 110 °C) was unveiled by 2D-HSQC NMR. The side-chain ( $\delta_{\rm C}/\delta_{\rm H}$  50.0-90.0/2.50-6.0 ppm) and aromatic ( $\delta_{\rm C}/\delta_{\rm H}$  100.0-150.0/9.0-5.5 ppm) regions of the CEL and recovered lignin, as well as the semiquantitative analysis, are listed in Fig. 5. The primary lignin cross-signal assignments of the 2D-HSQC spectra are referred to previous publication (Shen et al., 2019).

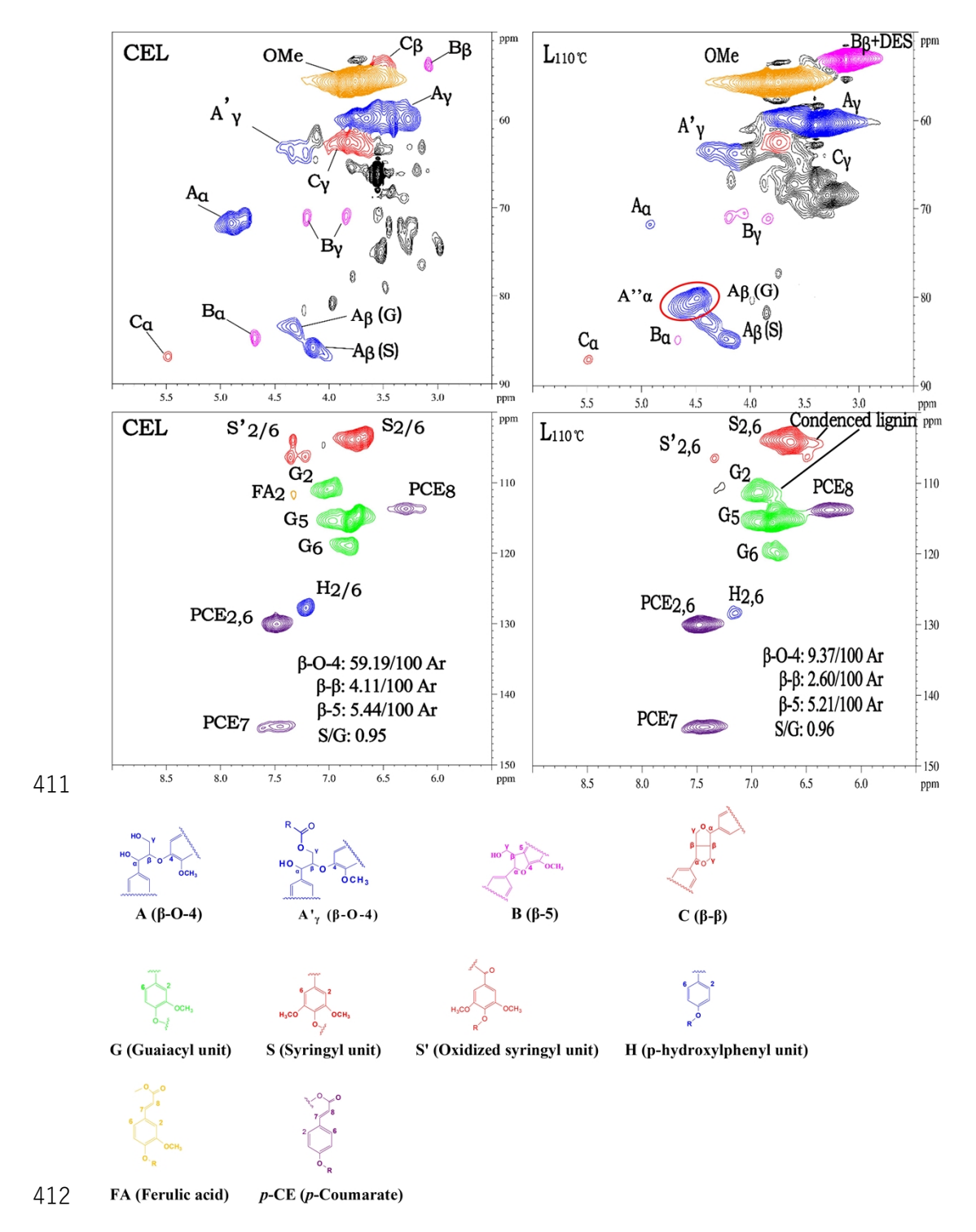


Fig. 5. Aromatic and side-chain regions of the CEL and L<sub>110 °C</sub> in the 2D HSQC
 NMR spectra.

In the side-chain region of the spectra (see Fig. 5), bamboo CEL had predominant signals of  $A_{\alpha}(\beta\text{-O-4})$ ,  $B_{\alpha}(\beta\text{-}\beta)$ , and  $C_{\alpha}(\beta\text{-}5)$  linkages at  $\delta_{C}/\delta_{H}$ 

415

417 71.62/4.85, 84.73/4.65, and 86.82/5.41 ppm. The  $\beta$ -position of  $A_{\beta}$  ( $\beta$ -O-4),  $B_{\beta}$ (β-β), and  $C_{\beta}$  (β-5) signals were centered at  $\delta_{C}/\delta_{H}$  86.1/4.05 ( $A_{\beta}$  for S) and 418 419 83.4/4.33 (A<sub>\beta</sub> for G), 53.5/3.05, and 52.4/3.45 ppm. The  $\gamma$ -position of A<sub>\gamma</sub> (\beta-O-4),  $B_{\nu}(\beta-\beta)$ , and  $C_{\nu}(\beta-5)$  signals were at  $\delta_{\rm C}/\delta_{\rm H}$  59.5/3.69, 71.0/4.16-3.79, and 420 421 62.3/3.70 ppm. Specifically, a new pronounced signal appeared at 80.05/4.49 422 ppm in the regenerated lignin (see red ring in Fig.5), which is reported to be 423 induced by the grafting of BDO on to the lignin structure (Liu et al., 2021). The semiquantitative data shows that the  $\beta$ -O-4 aryl ether content in CEL was 424 425 59.19/100 Ar, and it dramatically decreased to 9.37/100 Ar after the DES 426 pretreatment, indicating that our DES led to severe β-O-4 linkages cleavage. In addition to the cleavage of β-O-4 linkages, other carbon-carbon (C-C) bonds 427 428 had also been partially cleaved, in which a 36.74% reduction of  $\beta$ - $\beta$  bond (from 4.11 to 2.60/100Ar) occurred, and the  $\beta$ -5 linkages had a negligible decrease 429 430 (from 5.44 to 5.21/100Ar). It should be noted that the cleavage of main 431 interlinkages such as the aryl ether bond is usually accompanied by 432 condensation reactions, which may impact lignin's hydrophobicity, as will be illustrated later. 433 434 In the aromatic regions of bamboo CEL, pronounced signals of syringyl (S), guaiacyl (G), and p-hydroxyphenyl (H) units were clearly recognized. The 435 436 oxidized syringyl units (S'), ferulic acid (FA), and p-coumaric acid (PCE) signals were also easily identified. For example, the cross-peak of S<sub>2.6</sub> was 437 438 centered at  $\delta_C/\delta_H$  104.0/6.72 ppm, and that of the oxidized S unit (S'<sub>2.6</sub>) was

found at  $\delta_{\rm C}/\delta_{\rm H}$  106.3/7.21 ppm. The signals belonging to guaiacyl (G) units were at  $\delta_C/\delta_H$  111.0/6.99 (G<sub>2</sub>), 114.8/6.68 (G<sub>5</sub>), and 119.1/6.80 ppm (G<sub>6</sub>). The p-hydroxyphenyl (H) signal appeared at  $\delta_{\rm C}/\delta_{\rm H}$  127.9/7.19 ppm (H<sub>2.6</sub>). After pretreatment, distinct signals shift of the S<sub>2.6</sub>, and G<sub>5</sub> cross-peaks were observed, indicating some condensation reactions occurred during the pretreatment (Shen et al., 2019). It has been reported that the C-5 of G units could readily react with the free positions in adjacent lignin units to form a condensed structure, while the condensed S units were probably generated between the  $C_{\alpha}$  position of the side chain in S units and other active positions in fractionated lignin units to form a new carbon-carbon bond (Shen et al., 2020), which would increase the hydrophobicity of the recovered lignin. We further calculated the condensed structure (volume integration of contours proportion to the total aromatic rings) and it shows that 9.10% S unit and 2.54% G unit suffered from condensation during the DES pretreatment. As to the signals of FA at  $\delta_{\rm C}/\delta_{\rm H}$  110.7/7.35 ppm (FA<sub>2</sub>) in CEL, it disappeared after the pretreatment, while the peaks associated with PCE at  $\delta_C/\delta_H$  130.2/7.48 ppm  $(PCE_{2.6}), \delta_C/\delta_H 144.8/7.51 \text{ ppm } (PCE_7), \delta_C/\delta_H 113.9/6.29 \text{ ppm } (PCE_8) \text{ could}$ still be identified. The S/G ratio of lignin remained nearly unchanged after pretreatment.

3.2.2 Synergetic generation of LMS

439

440

441

442

443

444

445

446

447

448

449

450

451

452

453

454

455

456

457

458

The morphology of the recovered lignin pretreated under different SLRs at 110 °C for 1 h and different temperatures under 1:4 SLR for 1h was observed with

FE-SEM. As shown in Fig. 6, raw bamboo CEL presented irregular agglomerates. Surprisingly, the recovered DES lignin all had a regular sphere-like shape that was clearly dispersed, and the surface of the lignin spheres was smooth and neat, different from previous DES lignins which featured block or flake-like shapes (Lou et al., 2019; Shen et al., 2020).

The morphology of the obtained lignin in our proposed DES system was then compared with typical ChCl/p-toluenesulfonic acid, ChCl/oxalic acid, and ChCl/lactic acid DES systems. As shown in Fig. S1, the morphology of the recovered lignin from ChCl/oxalic acid (Fig. S1, a1-a3) and ChCl/lactic acid (Fig. S1, c1-c3) exhibited an irregular shape which is covered by a large amount of lignin debris. Besides, the recovered lignin using ChCl/p-toluenesulfonic acid system showed irregular morphology, similar to that of CEL. While in our BDO DES and other polyol-based DES (such as glycol, glycerol, and propanediol based DES), the recovered lignin all exhibited a regular LMS (Fig. 6 and Fig. S2). This result indicated that our polyol-based DES system could in one-pot obtain a tailored LMS after simple DES cooking, which will emancipate the low yield, complex process, and high cost in traditional LMS preparation processes (Ma et al., 2019), and facilitate the LMS valorization in adsorbent, ultraviolet screening agent, antioxidant, electrode materials, gas separator, catalyst, and other fields (Österberg et al., 2020).

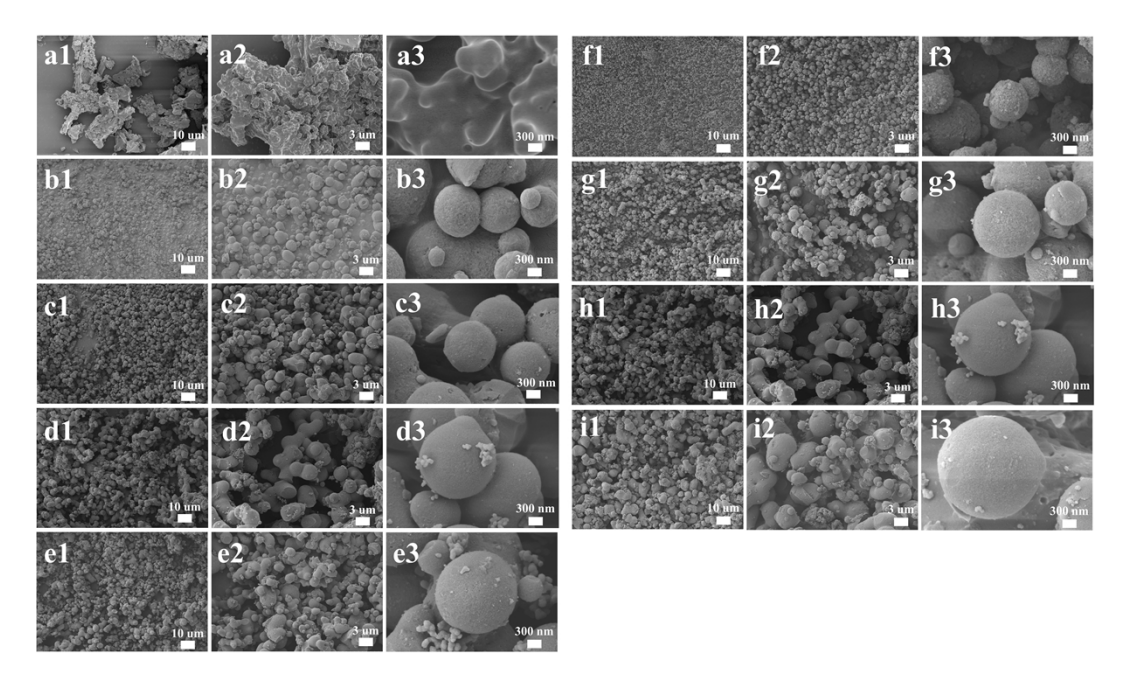


Fig. 6. SEM of CEL (a1-a3) and recovered lignin from different SLRs of L<sub>1:1</sub> (b1-b3),

- $L_{1:2}$  (c1-c3),  $L_{1:4}$  (d1-d3),  $L_{1:8}$  (e1-e3), and temperatures of  $L_{90}$  (f1-f3),  $L_{100}$  (g1-g3),
- $L_{110}$  (h1-h3) and  $L_{120 \, {}^{\circ}\text{C}}$  (i1-i3).
  - 3.2.3 Tailored LMS and its possible forming mechanism

After pretreatment under different SLRs at 110 °C for 1 h and different temperatures under 1:4 SLR for 1h, the size of the recovered LMS was also analyzed by a Zeta-sizer. As shown in Fig. 7a and b, the diameter of LMS was in several microns, and it tends to increase with the decrease of both SLR (1588-5239 nm) and the increase of temperature (1100-6192 nm). This result indicated that the lignin size could be regulated by changing the pretreatment condition. Interestingly, the diameter of the LMS was found to have a strong negative correlation with the M<sub>w</sub> (Fig. S3), indicating the small lignin debris are more prone to aggregate with each other, facilitating the formation of large LMS. This result is consistent with the previous publications, which reported that the formation mechanism of lignin particles

depended on the molecular weight and solubility of lignin (Zwilling et al., 2021). To further investigate the formation mechanism of lignin microspheres, the hydrophobicity of the recovered lignin was then determined (see Fig. 7c and d). At low temperatures (90-110 °C) and high SLR (1:1-1:4), the hydrophobicity was almost unchanged, keeping at a very low value (<0.5 L/g). Further changing the pretreatment parameters (e.g., high temperature and low SLR) significantly increased the hydrophobicity of lignin, which could be ascribed to the occurrence of some lignin condensation at these conditions that formed the carbon-carbon linkages and increased lignin's hydrophobicity. It can be seen that the diameter of the LMS had a positive relationship with its hydrophobicity which is contradictory to other studies using the traditional antisolvent method (Ma et al., 2020). This result indicated that hydrophobicity might be one of the main driving forces for the LMS generation in our proposed DES system. The polyol grating onto the  $\alpha$  position of lignin side chains (see 2 D HSQC NMR analysis section) could change the lignin structure and its hydrophobicity, which might also play an important role in facilitating the formation of the LMS. The BDO grafting reaction could significantly protect the lignin from further degradation (Cheng et al., 2022), resulting in an intact lignin structure which has a more hydrophilic sidechain, thus might increase the stability of the hydrophobic core at the same time strengthen the growing process induced by the hydrophilia shell. A possible mechanism of the lignin microsphere formation was proposed (Fig. S4). After introducing water to the lignin-rich DES pretreatment liquid, lignin nuclei were formed through aggregating the large molecular and homogenous hydrophobic lignin,

495

496

497

498

499

500

501

502

503

504

505

506

507

508

509

510

511

512

513

514

515

then the nuclei gradually grew by adsorbing the small particles composed of hydrophobic nuclei and hydrophilic shell. This path suggests that the small debris generated from the cleavage of the lignin's molecular chain would facilitate the lignin particle's growth under lower SLR and high temperatures. This hypothesis enabled an in-depth understanding of the formation of lignin spheres.

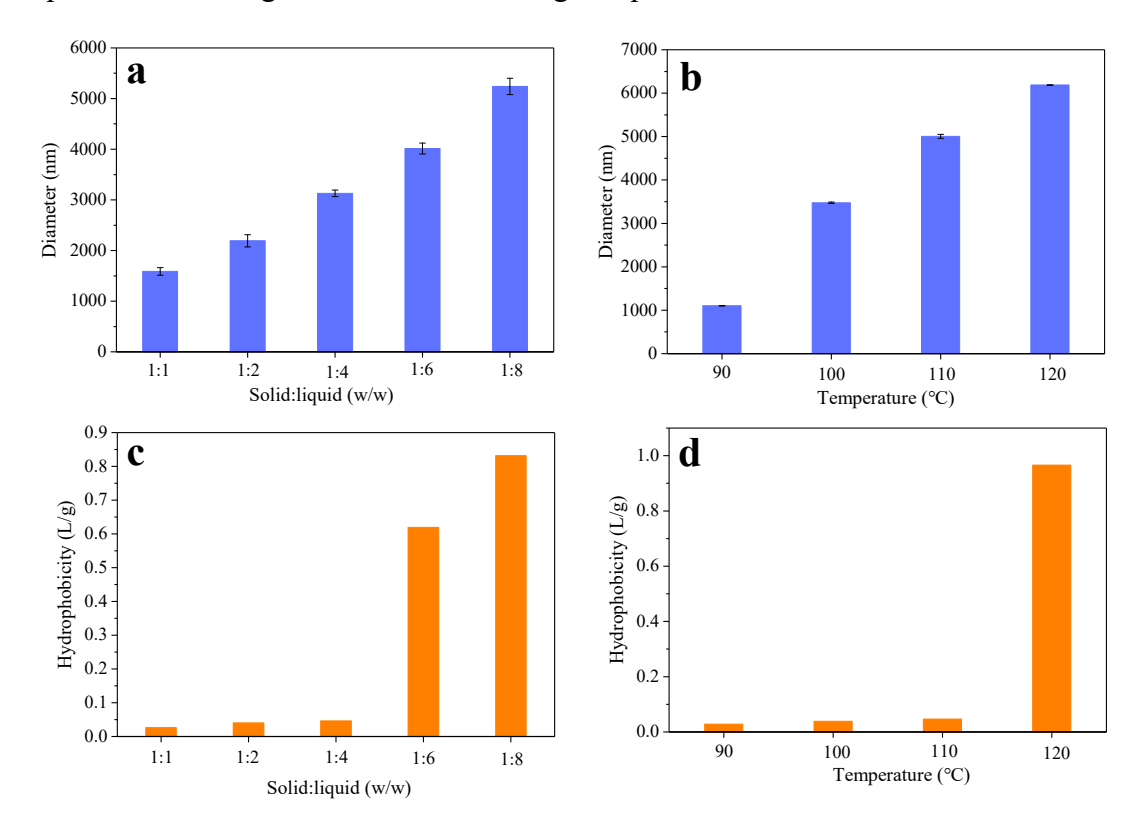


**Fig. 7.** Diameters (a,b) and hydrophobicity (c,d) of the recovered lignins under different SLRs at 110 °C and temperatures under 1:4 SLR.

# 3.3 Adsorption property analysis of the recovered LMS

One of the most critical applications of the LMS is their ability to be used as a recyclable dye adsorbent; thus, the utilization of LMS for the RhB dye scavenging from an aqueous solution was assessed in our study. The rate of the adsorption process is an essential factor that could determine the feasibility of using the sorbent

in large-scale industrial applications. The relationship between the time and the amount of dye adsorbed was studied. As shown in Fig. S5, more than 60% of the equilibrium adsorption capacity for RhB occurred within the first 50 min, indicating its high efficiency. The LMS adsorption rate was found to decrease gradually with decreasing the SLR (the LMS diameter increased from 1588 to 5239 nm). Specifically, the pretreatment efficiency increased as the SLR decreasing which resulted in the Mw decrease, the increase of hydrophobicity and the grafted diol tail decrease (Cheng et al., 2022). The decreased Mw means the increased lignin fragmentation, thus may lead to more growing reaction during the LMS formation process (Ma et al., 2020), resulting in a larger diameter and a poor adsorption performance. Besides, the increased hydrophobicity induced by the condensed reactions and the decrease of the grafted BDO might gather more lignin debris during the nucleation process, which also increased the diameter of the LMS. To investigate the kinetic mechanism, the pseudo-first-order and the pseudo-second-order equations were adopted to describe the adsorption processes (see Fig. S6).

The pseudo-first-order model (Li et al., 2021, 2016) was given as

The pseudo-second-order model (Li et al., 2021, 2016) was given as

$$\frac{t}{q_t} = \frac{1}{K_2 q_e^2} + \frac{t}{q_e}$$

530

531

532

533

534

535

536

537

538

539

540

541

542

543

544

551

Where K<sub>1</sub> and K<sub>2</sub> are the rate constant, q<sub>t</sub> and q<sub>e</sub> are the amounts of RhB adsorption at time t and at equilibrium (Li et al., 2016).

The correlation coefficients of the pseudo-first-order and the pseudo-second-

order model are listed in Table S2. It can be seen that the pseudo-second-order model had a higher  $R^2$  value than that of the pseudo-first-order model, and the calculated  $q_e$  values were also closer to the experimental data. This implied that the adsorption process of RhB on LMS was dominated by chemisorption, rather than diffusion (Li et al., 2016).

The adsorption capacity strongly correlates with its surface areas (Wu et al., 2021), and the LMS recovered from our system would be superior to other shapes because of the higher surface area. As shown in Fig. 8a, the RhB adsorption on LMS was gradually decreased from 55.05 mg/g (1:1 SLR) to 50.48 (1:2 SLR), 42.05 (1:4 SLR), 32.24 (1:6 SLR), and 31.64 mg/g (1:8 SLR). Obviously, the LMS could effectively adsorb the dyes of Rhodamine B, which outperformed some traditional materials relating to RhB adsorption with maximum value of 12.41 mg/g by biochar (Li et al., 2021) and 17.62 mg/g by Magnetic hollow microspheres (Li et al., 2016), indicating that our LMS had excellent property in removing organic RhB dyes from water. As shown in Fig. 8b, the adsorption ability of the recovered lignin had a strong relationship with the diameter of the LMS (R<sup>2</sup>=0.9336), which indicated that the surface areas of the recovered lignin governed the adsorption process.

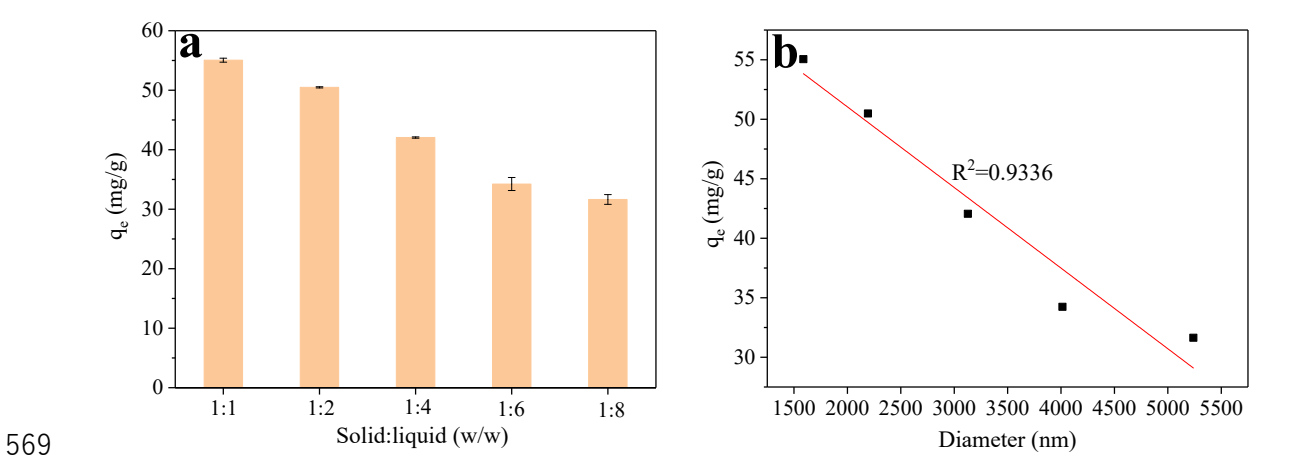


**Fig. 8.** The adsorption capability  $(q_e)$  at different SLRs (a) at 110 °C and the relationship between the diameter of LMS and its adsorption ability  $(q_e)$  (b). 3.4 DES reusability assessment

The recyclability of the DES has been considered a vital factor in promoting the cost-effective and eco-friendly DES-based lignocellulose pretreatment. It is reported that the weakening of DES usually occurred in DES recycling (Wang and Lee, 2021). For example, Xie et al (Xie et al., 2021) have studied a BTEAC/FA system which could only result in 66.6% lignin yield with only 76.6% enzymatic hydrolysis yield at a severe pretreatment temperature of 150 °C and 2 h. Zhu et al. (Chen et al., 2018b) also performed three pretreatment circles which showed remarkable weakened pretreatment effects with an 25.66% lignin removal and 32.6% glucan digestibility. Comparing with these poor performances, as shown in Fig. S7, our DES exhibited outstanding recyclability and pretreatment ability even after 7th cycles (over 90% DES was recovered throughout the seven circles). The pretreatment performance represented by lignin removal and enzymatic saccharification yield was also studied. The lignin removal maintained around 70% in 2-4 cycles, then it significantly

declined and reached 42.78% after the 7<sup>th</sup> circulation. Notably, the 72-h enzymatic saccharification yields of glucan and xylan still reached 100% even after 7<sup>th</sup> circulation (see Fig. S8). The high DES recovery and its excellent fractionation ability will realize a renewable and sustainable biorefinery process.

#### 3.5 Mass balance

The mass balance based on 1000 g feedstock under the optimal condition (110 °C, 1:4 SLR) is shown in Fig. 9. After the pretreatment, 592.40 g solid residue could be recovered, which contained 368.02 g glucan, 33.01 g xylan, and 87.78 g lignin, indicating the significant removal of lignin and xylan during the pretreatment. The following enzymatic hydrolysis yielded 404.91 g glucose and 36.67 g xylose, and it can be used to produce various fuels and chemicals. It should be noted that certain amount of unknown hemicellulose degradation products existed in the pretreatment liquid, which is hard to be identified and quantified. Besides, 196.28 g LMS could be directly obtained from the liquid phase as a coproduct, suggesting a high lignin yield of 97.11%. The DES could easily be separated from the liquid phase by evaporating the water and then reusing it, making the process renewable and sustainable.

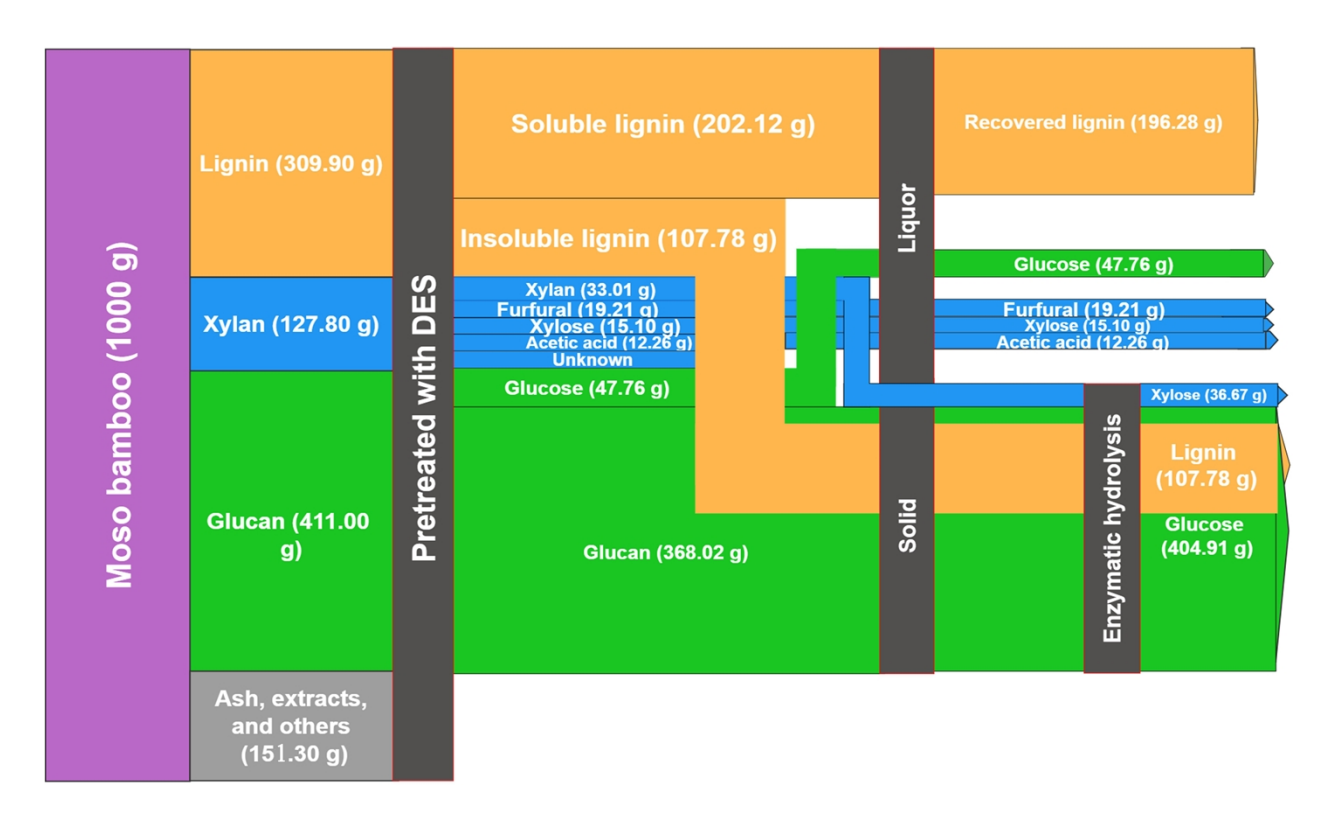


Fig. 9. Mass balance schematic diagram of the proposed DES biorefinery sequence.

# 3.6 Greenness evaluation by GAPI parameters

Green Analytical Procedure Index (GAPI) was first introduced by Płotka-Wasylka (Płotka-Wasylka, 2018) to assess the green character of the entire analytical methodology. GAPI can well evaluate the green character of an entire analytical methodology from sample collection to final determination, which not only provides an immediate perceptible perspective to the user/reader but also offers exhaustive information on evaluated procedures. The outcome is a pictogram with several fields related to sample processing, sample preparation, amount and nature of chemicals, energy, and waste. A simple outlook at the GAPI pictogram can reveal the green index of the procedure and the areas which require further improvement in terms of greenness (Ahmed and Abdallah, 2020). We systematically evaluated our procedures according to the "Green Analytical Procedure Index parameters description" referred

to the previous publication (Sánchez-Camargo et al., 2019). In brief, the greenness can be evaluated by a pictogram (with five pentagrams) from green through yellow to red representing low, medium to high environmental impact (Fig. 10). As shown in Table S3, the pictogram involves each step evaluation of the possible procedures such as collection (1), scale of extraction (6), health hazard (11) or waste treatment (15).

Our DES pretreatment processes used nontoxic solvent of BDO, ChCl and AlCl<sub>3</sub> and low-toxic acetone, which can be classified as green solvents/regents (7), slightly toxic and irritant (10) and no special hazards (11). During the pretreatment, we applied high-solid loading using an amount of 10-100 mL (10-100 g) (9) and low energy consumption with no more than 1.5 kWh (12). Remarkably, all the solvents could be recovered with a high recovery yield over 90% (15), thus the waste was <1 mL (<1 g) (14) throughout the pretreatment. After above GAPI analysis, green and yellow portions account for nearly total of the pictogram, indicating our DES process was green enough to make this biorefinery sustainable.

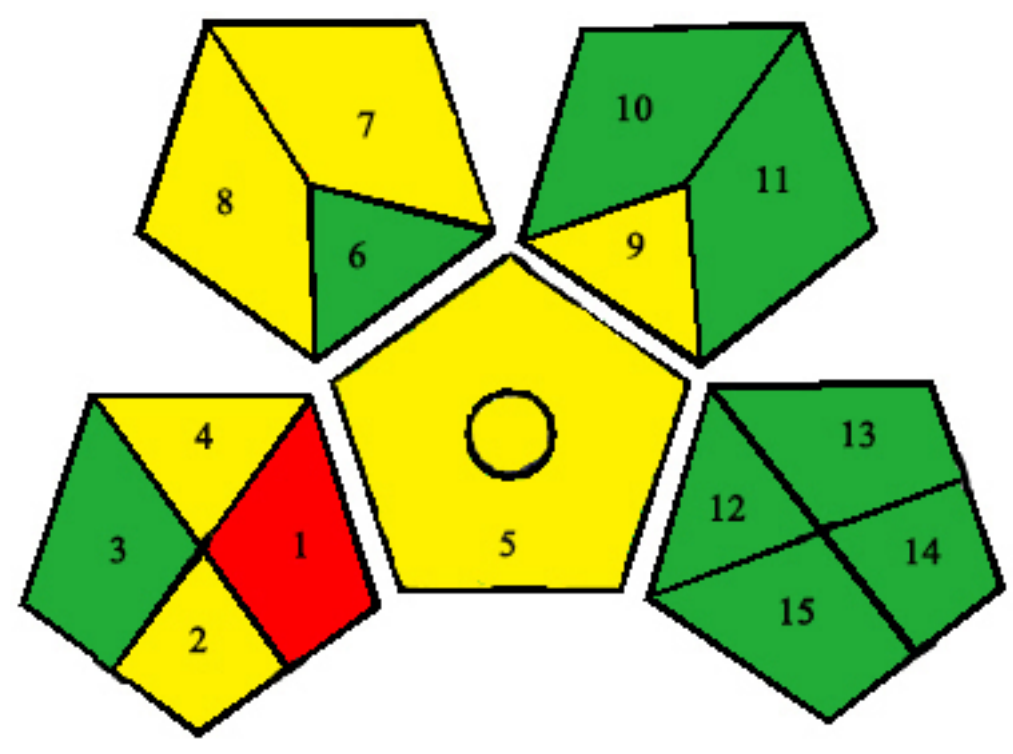


**Fig. 10.** GAPI assessment of the green profile of the evaluated procedures for the DES pretreatment.

#### 4. Conclusions

This work demonstrated the synergistic products of digestible substrate and LMS using a one-step DES pretreatment at low temperature and high solid loading. Results showed that ~70% lignin removal with over 90% lignin recovery yield could be achieved at the optimized condition. A 100% enzymatic saccharification was obtained after the pretreatment. Recyclability of the DES solution demonstrated over 90% DES could be recovered, and its pretreatment efficiency representing by the lignin removal (42.78%-87.66%) and glucan enzymatic saccharification (100%) was still highly maintained even after 7 times recycling process. Notably, the recovered lignins exhibited a quite regular micro-spherical morphology with a controllable diameter varying from 1100 to 6182 nm. Overall, the novel strategy offers a new biorefinery paradigm for the generation of various products in one pot which could contribute to

646	establish a green and sustainable biorefinery sequence from both the economic and
647	ecologic incentives.
648	Declaration of Competing Interest
649	There are no conflicts to declare.
650	Acknowledgments
651	This work was supported by Jiangsu Province Key Laboratory of Biomass
652	Energy and Materials (JSBEM-S-202203), Young Elite Scientist Sponsorship
653	Program by CAST, National Natural Science Foundation for Youth
654	(32001273), and Taishan Industrial Experts Programme (tscy20200213). AJR
655	and XM efforts were supported by the University of Tennessee, Knoxville.
656	
657	References:
658	Abu-Omar, M.M., Barta, K., Beckham, G.T., Luterbacher, J.S., Ralph, J., Rinaldi, R.,
659	Román-Leshkov, Y., Samec, J.S.M., Sels, B.F., Wang, F., 2021. Guidelines for
660	performing lignin-first biorefining. Energy Environ. Sci. 14, 262–292.
661	https://doi.org/10.1039/d0ee02870c
662	Ahmed, R., Abdallah, I., 2020. Development and Greenness Evaluation of
663	Spectrofluorometric Methods for Flibanserin Determination in Dosage Form and
664	Human Urine Samples. Molecules 25, 4932.
665	https://doi.org/10.3390/molecules25214932
666	Ai, B., Li, W., Woomer, J., Li, M., Pu, Y., Sheng, Z., Zheng, L., Adedeji, A.,
667	Ragauskas, A.J., Shi, J., 2020. Natural deep eutectic solvent mediated extrusion
668	for continuous high-solid pretreatment of lignocellulosic biomass. Green Chem.
669	22, 6372-6383. https://doi.org/10.1039/d0gc01560a
670	Chen, L., Shi, Y., Gao, B., Zhao, Y., Jiang, Y., Zha, Z., Xue, W., Gong, L., 2020.
671	Lignin Nanoparticles: Green Synthesis in a γ - Valerolactone/Water Binary

- Solvent and Application to Enhance Antimicrobial Activity of Essential Oils.
- https://doi.org/10.1021/acssuschemeng.9b06716
- 674 Chen, Z., Bai, X., Lusi, A., Wan, C., 2018a. High-Solid Lignocellulose Processing
- Enabled by Natural Deep Eutectic Solvent for Lignin Extraction and Industrially
- Relevant Production of Renewable Chemicals. ACS Sustain. Chem. Eng. 6,
- 677 12205–12216. https://doi.org/10.1021/acssuschemeng.8b02541
- 678 Chen, Z., Reznicek, W.D., Wan, C., 2018b. Deep eutectic solvent pretreatment
- enabling full utilization of switchgrass. Bioresour. Technol. 263, 40–48.
- https://doi.org/10.1016/j.biortech.2018.04.058
- 681 Cheng, J., Huang, C., Zhan, Y., Han, S., Wang, J., Meng, X., Geun Yoo, C., Fang, G.,
- Ragauskas, A.J., 2022. Effective biomass fractionation and lignin stabilization
- using a diol DES system. Chem. Eng. J. 443, 136395.
- https://doi.org/10.1016/j.cej.2022.136395
- 685 Guo, Z., Zhang, Q., You, T., Zhang, X., Xu, F., Wu, Y., 2019. Short-time deep
- eutectic solvent pretreatment for enhanced enzymatic sacchari fi cation and
- lignin. Green Chem. 21, 3099–3108. https://doi.org/10.1039/c9gc00704k
- Hong, S., Shen, X.J., Xue, Z., Sun, Z., Yuan, T.Q., 2020. Structure-function
- relationships of deep eutectic solvents for lignin extraction and chemical
- transformation. Green Chem. 22, 7219–7232.
- 691 https://doi.org/10.1039/d0gc02439b
- Huang, C., Zhan, Y., Cheng, J., Wang, J., Meng, X., Zhou, X., Fang, G., Ragauskas,
- A.J., 2021. Bioresource Technology Facilitating enzymatic hydrolysis with a
- novel guaiacol-based deep eutectic solvent pretreatment. Bioresour. Technol.
- 695 326, 124696. https://doi.org/10.1016/j.biortech.2021.124696
- Lancefield, C.S., Panovic, I., Deuss, P.J., Barta, K., Westwood, N.J., 2017. Pre-
- treatment of lignocellulosic feedstocks using biorenewable alcohols: Towards
- complete biomass valorisation. Green Chem. 19, 202–214.
- 699 https://doi.org/10.1039/c6gc02739c
- Li, X., Shi, J., Luo, X., 2021. Enhanced adsorption of rhodamine B from water by Fe-

- N co-modified biochar: Preparation, performance, mechanism and reusability.
- 702 Bioresour. Technol. 343, 126103. https://doi.org/10.1016/j.biortech.2021.126103
- Li, Y., Wu, M., Wang, B., Wu, Y., Ma, M., Zhang, X., 2016. Synthesis of Magnetic
- Lignin-Based Hollow Microspheres: A Highly Adsorptive and Reusable
- Adsorbent Derived from Renewable Resources. ACS Sustain. Chem. Eng. 4,
- 706 5523–5532. https://doi.org/10.1021/acssuschemeng.6b01244
- Ling, Z., Tang, W., Su, Y., Shao, L., Wang, P., Ren, Y., Huang, C., 2021. Bioresource
- 708 Technology Promoting enzymatic hydrolysis of aggregated bamboo crystalline
- cellulose by fast microwave-assisted dicarboxylic acid deep eutectic solvents
- pretreatments. Bioresour. Technol. 333, 125122.
- 711 https://doi.org/10.1016/j.biortech.2021.125122
- Liu, Y., Deak, N., Wang, Z., Deuss, P.J., Barta, K., Yu, H., Hameleers, L., Jurak, E.,
- 713 2021. Tunable and functional deep eutectic solvents for lignocellulose
- valorization. Nat. Commun. 12, 5452. https://doi.org/10.1038/s41467-021-
- 715 25117-1
- Lou, R., Ma, R., Lin, K.T., Ahamed, A., Zhang, X., 2019. Facile Extraction of Wheat
- 717 Straw by Deep Eutectic Solvent (DES) to Produce Lignin Nanoparticles. ACS
- 718 Sustain. Chem. Eng. 7, 10248–10256.
- 719 https://doi.org/10.1021/acssuschemeng.8b05816
- Ma, M., Dai, L., Si, C., Hui, L., Liu, Z., Ni, Y., 2019. A Facile Preparation of Super
- 721 Long-Term Stable Lignin Nanoparticles from Black Liquor. ChemSusChem
- 722 5239 –5245. https://doi.org/10.1002/cssc.201902287
- Ma, M., Dai, L., Xu, J., Liu, Z., Ni, Y., 2020. A simple and effective approach to
- fabricate lignin nanoparticles with tunable sizes based on lignin fractionation.
- 725 Green Chem. 22, 2011–2017. https://doi.org/10.1039/d0gc00377h
- Mankar, A.R., Pandey, A., Modak, A., Pant, K.K., 2021. Bioresource Technology
- Pretreatment of lignocellulosic biomass : A review on recent advances.
- 728 Bioresour. Technol. 334, 125235. https://doi.org/10.1016/j.biortech.2021.125235
- Modenbach, A.A., Nokes, S.E., 2012. The Use of High-Solids Loadings in Biomass

- 730 Pretreatment A Review. Biotechnol. Bioeng. 109, 1430–1442.
- 731 https://doi.org/10.1002/bit.24464
- Österberg, M., Sipponen, M.H., Mattos, B.D., Rojas, O.J., 2020. Spherical lignin
- particles: A review on their sustainability and applications. Green Chem. 22,
- 734 2712–2733. https://doi.org/10.1039/d0gc00096e
- Pan, Z., Li, Y., Wang, B., Sun, F., Xu, F., Zhang, X., 2021. Mild fractionation of
- poplar into reactive lignin via lignin-first strategy and its enhancement on
- 737 cellulose saccharification. Bioresour. Technol. 343, 126122.
- 738 https://doi.org/10.1016/j.biortech.2021.126122
- 739 Pang, T., Wang, G., Sun, H., Wang, L., Liu, Q., Sui, W., Parvez, A.M., Si, C., 2020.
- Lignin Fractionation for Reduced Heterogeneity in Self-Assembly Nanosizing:
- Toward Targeted Preparation of Uniform Lignin Nanoparticles with Small Size.
- 742 ACS Sustain. Chem. Eng. 8, 9174–9183.
- https://doi.org/10.1021/acssuschemeng.0c02967
- Płotka-Wasylka, J., 2018. A new tool for the evaluation of the analytical procedure:
- Green Analytical Procedure Index. Talanta 181, 204–209.
- 746 https://doi.org/10.1016/j.talanta.2018.01.013
- Provost, V., Dumarcay, S., Ziegler-Devin, I., Boltoeva, M., Trébouet, D., Villain-
- Gambier, M., 2022. Deep eutectic solvent pretreatment of biomass: Influence of
- hydrogen bond donor and temperature on lignin extraction with high  $\beta$ -O-4
- content. Bioresour. Technol. 349. https://doi.org/10.1016/j.biortech.2022.126837
- Ragauskas, A.J., Beckham, G.T., Biddy, M.J., Chandra, R., Chen, F., Davis, M.F.,
- Davison, B.H., Dixon, R.A., Gilna, P., Keller, M., Langan, P., Naskar, A.K.,
- Saddler, J.N., Tschaplinski, T.J., Tuskan, G.A., Wyman, C.E., 2014. Lignin
- valorization: Improving lignin processing in the biorefinery. Science. 344,
- 755 1246843. https://doi.org/10.1126/science.1246843
- Sánchez-Camargo, A. del P., Bueno, M., Parada-Alfonso, F., Cifuentes, A., Ibáñez,
- E., 2019. Hansen solubility parameters for selection of green extraction solvents.
- 758 TrAC Trends Anal. Chem. 118, 227–237.

- 759 https://doi.org/10.1016/j.trac.2019.05.046
- Shen, X., Chen, T., Wang, H., Mei, Q., Yue, F., Sun, S., 2020. Structural and
- Morphological Transformations of Lignin Macromolecules during Bio-Based
- Deep Eutectic Solvent (DES) Pretreatment. ACS Sustain. Chem. Eng. 8, 2130–
- 763 2137. https://doi.org/10.1021/acssuschemeng.9b05106
- 764 Shen, X., Wen, J., Mei, Q., Chen, X., Sun, D., Yuan, T., Sun, R., 2019. Facile
- fractionation of lignocelluloses by biomass-derived deep eutectic solvent (DES)
- pretreatment for cellulose enzymatic hydrolysis and lignin valorization. Green
- 767 Chem. 21, 275–283. https://doi.org/10.1039/c8gc03064b
- Sirviö, J.A., Visanko, M., Liimatainen, H., 2016. Acidic Deep Eutectic Solvents As
- Hydrolytic Media for Cellulose Nanocrystal Production. Biomacromolecules 17,
- 770 3025–3032. https://doi.org/10.1021/acs.biomac.6b00910
- 771 Sluiter, A., Hames, B., Ruiz, R., Scarlata, C., Sluiter, J., Templeton, D., Crocker, D.,
- 772 2012. Determination of structural carbohydrates and lignin in Biomass -
- 773 NREL/TP-510-42618. Lab. Anal. Proced. 17.
- Wang, W., Lee, D.J., 2021. Lignocellulosic biomass pretreatment by deep eutectic
- solvents on lignin extraction and saccharification enhancement: A review.
- 776 Bioresour. Technol. 339, 125587. https://doi.org/10.1016/j.biortech.2021.125587
- Wang, Y., Meng, X., Jeong, K., Li, S., Leem, G., Kim, K.H., Pu, Y., Ragauskas, A.J.,
- Yoo, C.G., 2020. Investigation of a Lignin-Based Deep Eutectic Solvent Using p
- -Hydroxybenzoic Acid for Efficient Woody Biomass Conversion. ACS Sustain.
- 780 Chem. Eng. 8, 12542–12553. https://doi.org/10.1021/acssuschemeng.0c03533
- Wang, Z.K., Hong, S., Wen, J. long, Ma, C.Y., Tang, L., Jiang, H., Chen, J.J., Li, S.,
- Shen, X.J., Yuan, T.Q., 2020. Lewis Acid-Facilitated Deep Eutectic Solvent
- 783 (DES) Pretreatment for Producing High-Purity and Antioxidative Lignin. ACS
- 784 Sustain. Chem. Eng. 8, 1050–1057.
- https://doi.org/10.1021/acssuschemeng.9b05846
- Wei, H.L., Bu, J., Zhou, S.S., Deng, M.C., Zhu, M.J., 2021. A facile ionic liquid and
- p-toluenesulfonic acid pretreatment of herb residues: Enzymatic hydrolysis and

- 788 lignin valorization. Chem. Eng. J. 419, 129616.
- 789 https://doi.org/10.1016/j.cej.2021.129616
- Wen, J.L., Sun, S.L., Yuan, T.Q., Sun, R.C., 2015. Structural elucidation of whole
- 791 lignin from Eucalyptus based on preswelling and enzymatic hydrolysis. Green
- 792 Chem. 17, 1589–1596. https://doi.org/10.1039/c4gc01889c
- Wu, H., Gong, L., Zhang, X., He, F., Li, Z., 2021. Bifunctional porous
- polyethyleneimine-grafted lignin microspheres for efficient adsorption of 2, 4-
- 795 dichlorophenoxyacetic acid over a wide pH range and controlled release. Chem.
- 796 Eng. J. 411, 128539. https://doi.org/10.1016/j.cej.2021.128539
- 797 Wu, X., Huang, Chen, Zhai, S., Liang, C., Huang, Caoxing, 2018. Bioresource
- 798 Technology Improving enzymatic hydrolysis e ffi ciency of wheat straw through
- sequential autohydrolysis and alkaline post-extraction. Bioresour. Technol. 251,
- 800 374–380. https://doi.org/10.1016/j.biortech.2017.12.066
- Xia, Q., Liu, Yongzhuang, Meng, J., Cheng, W., Chen, W., Liu, S., Liu, Yixing, Li,
- J., Yu, H., 2018. Multiple hydrogen bond coordination in three-constituent deep
- eutectic solvents enhances lignin fractionation from biomass. Green Chem. 20,
- 804 2711–2721. https://doi.org/10.1039/c8gc00900g
- Xie, J., Chen, J., Cheng, Z., Zhu, S., Xu, J., 2021. Pretreatment of pine lignocelluloses
- by recyclable deep eutectic solvent for elevated enzymatic saccharification and
- lignin nanoparticles extraction. Carbohydr. Polym. 269, 118321.
- 808 https://doi.org/10.1016/j.carbpol.2021.118321
- 809 Xu, L., Zhang, S.J., Zhong, C., Li, B.Z., Yuan, Y.J., 2020. Alkali-Based Pretreatment-
- Facilitated Lignin Valorization: A Review. Ind. Eng. Chem. Res. 59, 16923–
- 811 16938. https://doi.org/10.1021/acs.iecr.0c01456
- Xu, Y., Zhou, Q., Li, M., Bian, J., Peng, F., 2019. Bioresource Technology
- Tetrahydro-2-furanmethanol pretreatment of eucalyptus to enhance cellulose
- enzymatic hydrolysis and to produce high-quality lignin. Bioresour. Technol.
- 815 280, 489–492. https://doi.org/10.1016/j.biortech.2019.02.088
- Zhang, Zhenlei, Lahive, C.W., Winkelman, J.G.M., Barta, K., Deuss, P.J., 2022.

817	Chemicals from lignin by diol-stabilized acidolysis: reaction pathways and
818	kinetics. Green Chem. 895–905. https://doi.org/10.1039/d2gc00069e
819	Zhang, Zhaohui, Xu, J., Xie, J., Zhu, S., Wang, B., Li, J., Chen, K., 2022.
820	Physicochemical transformation and enzymatic hydrolysis promotion of reed
821	straw after pretreatment with a new deep eutectic solvent. Carbohydr. Polym.
822	290, 119472. https://doi.org/10.1016/j.carbpol.2022.119472
823	Zwilling, J.D., Jiang, X., Zambrano, F., Venditti, R.A., Jameel, H., Velev, O.D.,
824	Rojas, O.J., Gonzalez, R., 2021. Understanding lignin micro- And nanoparticle
825	nucleation and growth in aqueous suspensions by solvent fractionation. Green
826	Chem. 23, 1001–1012. https://doi.org/10.1039/d0gc03632c
827	